

# Anomalous phase behavior of long chain saturated lecithin bilayers

W.-J. Sun <sup>a</sup>, S. Tristram-Nagle <sup>b</sup>, R.M. Suter <sup>a</sup>, J.F. Nagle <sup>a,b,\*</sup>

<sup>a</sup> Department of Physics, Carnegie Mellon University, Pittsburgh, PA 15213, USA

<sup>b</sup> Department of Biological Sciences, Carnegie Mellon University, Pittsburgh, PA 15213, USA

Received 19 June 1995; accepted 20 September 1995

## Abstract

X-ray scattering has been performed on fully hydrated unoriented multilamellar vesicles of lecithins with even chain lengths  $n$  from 16 to 24 as a function of temperature in chain ordered phases. The longer chain lengths,  $n \geq 20$ , show anomalous behavior compared to the shorter chain lengths,  $n < 20$ . This report concentrates on  $n = 24$ . Although the history and time dependence shows that equilibrium was not always achieved, it appears that there is a second gel-like phase G2 below 40°C. The G2 phase has a small tilt angle and opposite hexagonal symmetry breaking from the usual G1 gel phase. Also, as  $T$  is raised above 45°C, the wide-angle data suggest the appearance of a phase with hexagonal chain packing and small chain tilt angle.

**Keywords:** Lipid bilayer; Phosphatidylcholine; X-ray scattering; Gel phase

## 1. Introduction

The study of lipid bilayers has been and will continue to be greatly enriched by investigating how the structure and thermodynamic properties vary as the lipids are varied, including both naturally occurring and specifically synthesized lipids. One particularly appropriate strategy is to vary the chain length [1–4], since this variation systematically alters the balance between the interactions involving the headgroups, which remain the same, and the total interactions between the chains, which increase with increasing chain length. This variation yields increased main transition temperatures with increased chain length [1–4]. It also may involve more subtle changes; e.g., decreasing chain length for the phosphatidylethanolamines alters the phase diagram from one having stable gel phases to one in which the gel phase is merely metastable at all temperatures [5].

In a recent study of a sequence of di-saturated phosphatidylcholines from this laboratory, it was found that the wide-angle pattern in the gel phase started to become qualitatively different as the chain length  $n$  was increased beyond 20 carbons [6]. When  $C_{22}$  and  $C_{24}$  chains were investigated, rather different wide-angle patterns were observed compared to those for shorter chain lengths  $14 < n$

$< 20$ , and so a detailed study of the longer chain lengths was not included in a previous report [6]. The purpose of the present study is to report some details of this anomalous behavior of the longer chain lecithins.

## 2. Materials and methods

All lecithins were purchased in lyophilized form from Avanti Polar Lipids (1,2-dipalmitoyl-*sn*-glycero-3-phosphatidylcholine (to be abbreviated  $C_{16}$ ) Lot# 160PC-188; 1,2-distearoyl-*sn*-glycero-3-phosphatidylcholine ( $C_{18}$ ) Lot# 180PC-76; 1,2-diarachidoyl-*sn*-glycero-3-phosphatidylcholine ( $C_{20}$ ) Lot# 200PC-17; 1,2-dibehenoyl-*sn*-glycero-3-phosphatidylcholine ( $C_{22}$ ) Lot# 220PC-24; 1,2-dilignoceroyl-*sn*-glycero-3-phosphatidylcholine ( $C_{24}$ ) Lot# 240PC-24) and used without further purification. Lipid/water dispersions were placed in 1 mm  $\times$  4 cm capillaries following standard procedures [6]. Upon brief centrifugation, these dispersions separate into a lipid-rich phase, from which X-ray scattering was performed, and a clear water-rich phase, thus demonstrating full hydration. The sealed sample was further annealed by incubating at 80–95°C overnight. Following scattering measurements, the lipid was dried under nitrogen and assayed for radiation and thermal damage by thin-layer chromatography using the solvent system chloroform/methanol/7 M ammonium hydroxide (46:18:3, v/v).

\* Corresponding author (at address a). Fax: +1 (412) 6810648.

The sample chamber is a custom-built aluminum can with ultrathin (1.5  $\mu\text{m}$ ) mylar windows. It holds a cassette with slots for 10 X-ray capillaries. The chamber is connected to a motorized 3D translational unit, which allows easy access of the X-ray beam to the capillaries and new spots on each capillary; this facilitates sample loading and allows us to minimize radiation damage by frequently translating unexposed sample into the beam. The temperature was monitored by a platinum resistance thermometer and temperature was automatically controlled through heating strips symmetrically arranged on the outside of the chamber in order to minimize the temperature gradient.

Our principle measurements were carried out using  $\text{Cu } K_{\alpha}$  X rays from a rotating anode source interfaced with a four-circle diffractometer and a Braun linear position sensitive detector (PSD) as previously described [7]. We used a graphite monochromator and a pair of  $xy$  slit sets to further restrict the beam size and divergence. Accounting for the finite beam size, the finite sample size and the divergence of the incoming beam leads to an estimate for the instrumental (longitudinal) resolution of  $0.075^{\circ}$  (HWHM) in  $2\theta$  or  $\Delta q = 5 \times 10^{-3} \text{ \AA}^{-1}$ . The maximum exposure time on one spot was about 4 h with X-ray power of 5.25 kW; no changes in the diffraction peaks were detected in this time. In addition, some film data were collected in 17 h using a Philips Norelco X-ray source at 0.2 kW. The beam was pinhole collimated with a sample-to-film distance of 66 mm, and Kodak DEF5 film was used.

### 3. Results

Fig. 1 shows wide-angle scattering data at  $25^{\circ}\text{C}$  for different chain lengths. For the shorter chain lengths ( $n \leq 20$ ) there is a sharp (20) peak and a broad (11) peak; this pattern is well understood to be due to the following properties of the chain packing [7–10]: (1) chains are packed in a centered rectangular (often called orthorhombic or distorted hexagonal) lattice; (2) chains are tilted towards nearest neighbors; (3) chains of the two opposing monolayers are parallel to each other, not pleated against each other; (4) and chains in different bilayers are not in registry. As  $n$  increases, the angular separation between the (20) and (11) peaks increases. For  $n = 24$  there are four peaks in Fig. 1; these will be labeled A through D. For  $n = 22$  there is a small peak that corresponds to peak B for  $n = 24$ ; under different conditions there is also a clearly visible peak for  $n = 22$  that corresponds to the D peak for  $n = 24$ , but it is too small to be seen in the data in Fig. 1. Following the systematic trend of the shorter chain lengths, Fig. 1 suggests that A and C are the (20) and (11) peaks from the usual chain tilted gel phase as in the shorter chain length lipids.

Fig. 2 shows the  $d$ -spacings  $d_{20}$  from peak A and  $d_{11}$  from peak C as a function of  $T$ . The systematic trend with

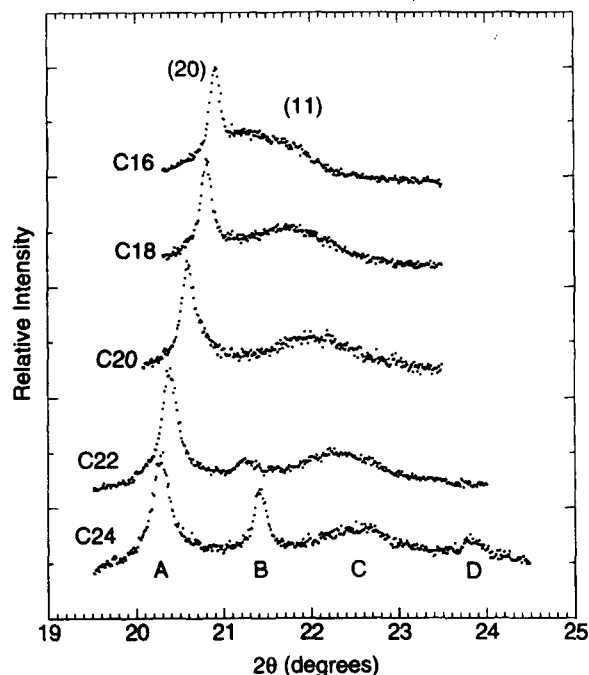


Fig. 1. Wide-angle scattering data at  $25^{\circ}\text{C}$  for different chain lengths. The (20) and (11) peaks are present in the usual tilted gel phase. The four peaks present in  $\text{C}_{24}$  are named A, B, C and D.

chain length  $n$  of these  $d$ -spacing curves supports the suggestion that the A and C peaks for  $n = 22$  and  $n = 24$  correspond to the usual gel phase. Quantitative analysis of the wide-angle spacings and additional aspects of this usual gel phase as a function of  $n$  and  $T$  will be discussed in detail in another paper.

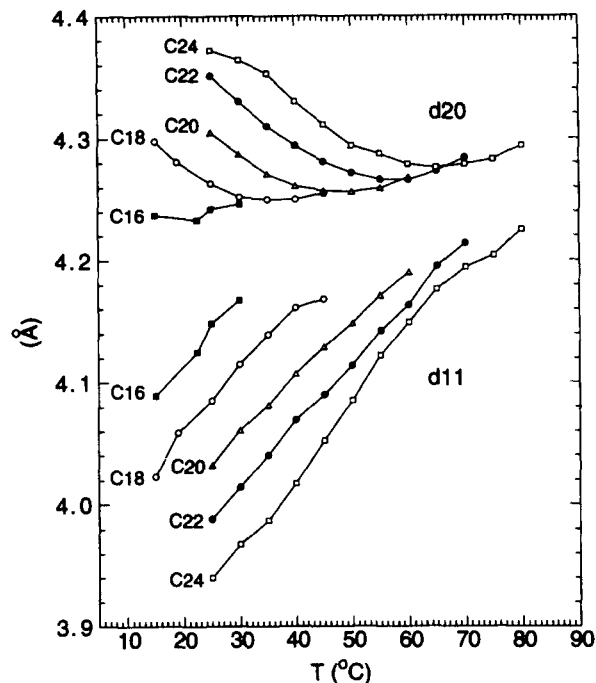


Fig. 2. Temperature and chain length dependence of the usual gel phase wide-angle spacings  $d_{11}$  and  $d_{20}$  in  $\text{Å}$ .

Let us now turn to a more quantitative characterization of the new B and D peaks shown in Fig. 1 and let us focus upon  $C_{24}$  for which the effect is more pronounced. Fig. 3 illustrates the variety of wide-angle scattering that can be obtained from nominally similar samples. Traces 1 and 2 in Fig. 3 were measured on the same sample, with the difference that the sample was heated to  $80^\circ\text{C}$  for 4 h between the two measurements. Trace 3 in Fig. 3 is from a sample that had been prepared by hydrating the lipid in the capillary and then annealing between  $5^\circ\text{C}$  and  $90^\circ\text{C}$  several times. These latter data show almost pure B and D peaks, but when this sample was heated to and held at  $80^\circ\text{C}$  and then brought back to  $25^\circ\text{C}$ , its wide-angle scattering more closely resembled trace 2 in Fig. 3. This suggests that trace 2 may be the more stable result. Most importantly, the data in Fig. 3 clearly show that the sizes of peaks B and D are proportional to each other and the sizes of peaks A and C are proportional to each other. However, the relative sizes of peaks A and B are clearly highly variable. This supports the identification of peaks A and C belonging to the usual gel phase that we will call G1 and peaks B and D belonging to a new phase that we will call G2.

Further support for identifying two coexisting phases comes from the temperature dependence of the wide-angle scattering in Fig. 4 which shows larger B and D peaks and smaller A and C peaks at the lower temperatures. As the temperature is increased, the ratio of the A and C peaks relative to the B and D peaks increases until there are only A and C peaks at  $40^\circ\text{C}$ . All of these data were obtained

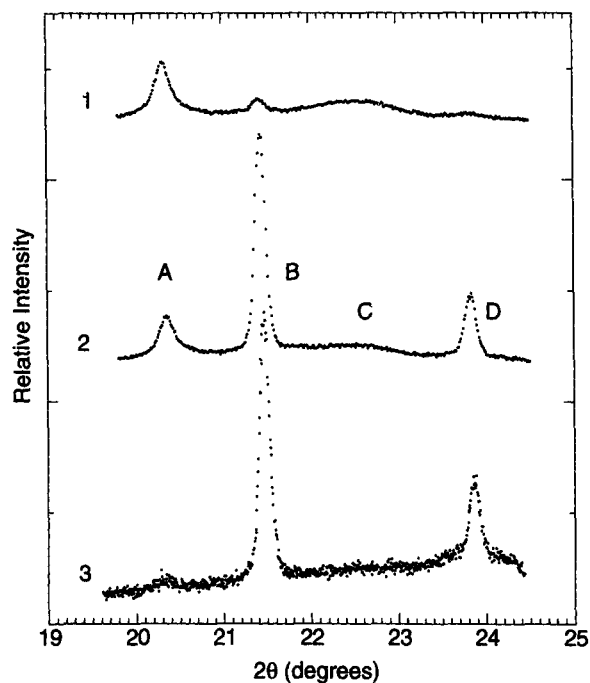


Fig. 3. Wide-angle scattering data from  $C_{24}$  at  $25^\circ\text{C}$ . Traces 1 and 2 are from the same sample, with the second trace taken after high temperature annealing for 4 h at  $80^\circ\text{C}$ . The third trace is from a different sample (described in the text).

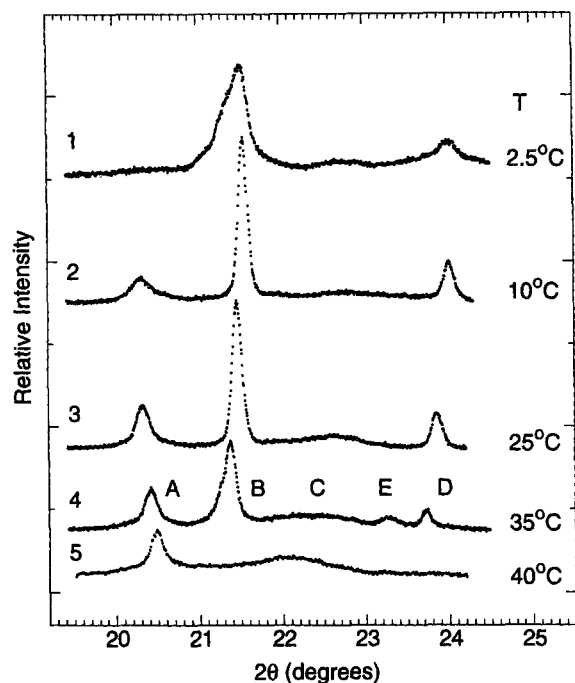


Fig. 4. Wide-angle data from  $C_{24}$  in the low-temperature regime. Peaks A and C belong to the usual G1 phase, while B and D peaks belong to a new phase, G2. The E peak is associated with the G1 phase.

from samples that had been raised to  $80^\circ\text{C}$  in the capillary, similar to trace 2 in Fig. 3. We note the appearance of an additional peak E shown in the data at  $35^\circ\text{C}$  in Fig. 4. The size of this E peak was proportional to the size of the A peak and decreased as the size of the B peak increased, although peak E was not always present when the sample was freshly prepared. When the temperature was only varied in the range below  $45^\circ\text{C}$ , the magnitudes of the wide-angle peaks were not so irreversible as in Fig. 3, and the irreversibility went in the opposite direction. Specifically, we observed a small increase in the A and C peaks relative to the B and D peaks (data not shown) (i) when a sample was maintained at  $35^\circ\text{C}$  after being heated to  $80^\circ\text{C}$  and (ii) when a sample was cycled from  $25^\circ\text{C}$  to  $40^\circ\text{C}$  and back to  $25^\circ\text{C}$ . However, we observed no change with time at  $25^\circ\text{C}$ , even when the total elapsed time was 33 h.

The A and C peaks have been identified as the (20) and (11) peaks of the usual tilted-chain gel phase G1. Since the phase associated with the B and D peaks becomes more prominent at lower temperature, one might guess that it is a subgel phase. Subgel phases have several additional weak diffraction rings at angles between 7 and 17 degrees [11–14]; these extra rings could be due to larger unit cells as well as to symmetry breaking between different chains in each unit cell so that, unlike the usual gel phase, peaks with an odd sum of the two in-plane indices would not have to be extinct. Fig. 5 shows film data for a sample with relatively stronger BD peaks compared to the AC peaks. This film does not show any weak rings between the low-angle lamellar rings and the ABCD rings, suggest-

ing that the BD phase is not a subgel phase. However, two extra very weak rings were observed at  $2\theta = 36.3^\circ$  and  $40.9^\circ$  in Fig. 5. These extra rings were weaker for samples with weaker BD peaks compared to the AC peaks (data not shown). Assuming an orthorhombic lattice and the more intense ring B as (11) plus  $(1\bar{1})$  and the less intense ring D as (20) yields lattice constants  $a = 7.45 \text{ \AA}$  and  $b = 4.97 \text{ \AA}$ ; then, the two extra weak rings nicely index as (31) and (02). The non-appearance of any rings with odd sums of indices suggests that the chains in the unit cell are still basically equivalent, as in the usual gel phase, so we classify the G2 phase as a second gel-like phase.

The sharpness of the B and D peaks suggests that the chains have little tilt relative to the bilayer normal [10,15]. The G2 phase has a more compact chain packing than the usual G1 gel phase; the area in the plane perpendicular to the chains is  $A_c = 18.5 \text{ \AA}^2$  at  $25^\circ\text{C}$ , smaller than for the usual gel phase which has  $A_c = 19.3 \text{ \AA}^2$  at  $25^\circ\text{C}$ . A notable difference between the G2 phase and the G1 phase is that the order of the (20) and (11) peaks is reversed. This means that, when compared to hexagonal packing of chains, the chains in the G2 phase are more compressed along the (10) direction (i.e., along a direction between two neighboring chains) whereas the chains in the usual gel phase are more compressed along the (01) direction (i.e., along a direction towards a neighboring chain).

It has been emphasized that there is a great deal of thermal hysteresis and sample preparation dependence (Fig. 3) in the scattering data taken below  $40^\circ\text{C}$ . We will also see additional complications above  $45^\circ\text{C}$ . In the midst of

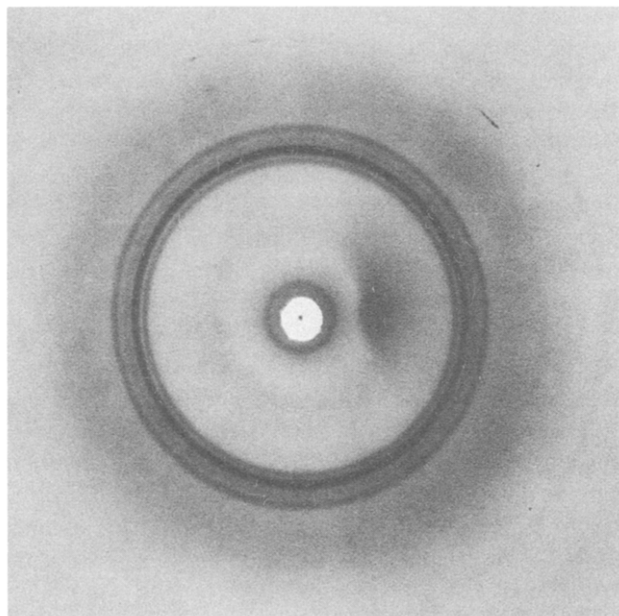


Fig. 5. Film data from  $C_{24}$  at  $22^\circ\text{C}$ . This sample had been raised to  $70^\circ\text{C}$  for 1 h and allowed to cool slowly to room temperature before this picture. The four prominent wide-angle rings shown in this film correspond to peaks A, B, C and D as described in the text. The shadow to the right of the beam was from scattering off the beam stop.

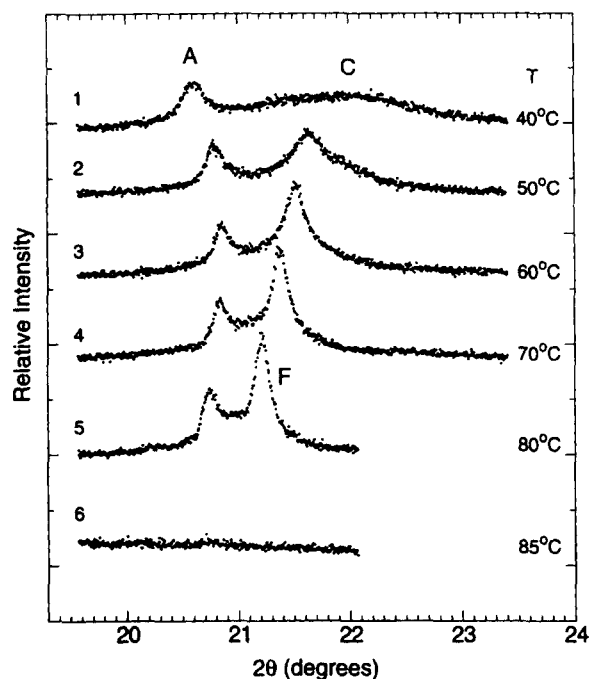


Fig. 6. Wide-angle data from  $C_{24}$  in the high-temperature regime. The F peak appears to be associated with a new phase, G3. Each trace was taken 2 h after the preceding one.

these complications, it is fortunate that there appears to be reproducibility for temperatures between 40 and  $45^\circ\text{C}$ , for which we always obtained a rather normal gel phase pattern with peaks A and C. This suggests that it is appropriate to split the study of  $C_{24}$  into two temperatures regimes. We now turn to the high-temperature regime,  $T > 45^\circ\text{C}$ .

The wide-angle data of the high-temperature regime are shown in Fig. 6. At  $85^\circ\text{C}$  this sample of  $C_{24}$  enters the fluid  $L_\alpha$  phase with only broad wide-angle scattering centered below  $20^\circ$ . For lower temperatures, it first appears that the broad C peak that occurs at  $40^\circ\text{C}$  in the G1 phase gradually sharpens as  $T$  is increased to  $80^\circ\text{C}$ . However, detailed peak fitting reveals a different interpretation that is shown in Fig. 7. Just as for the shorter chain lengths, the broad C peak moves close to the sharp A peak with increasing temperature, and the C peak remains broad as for the shorter chain lengths. In addition, a new sharp peak that we will call the F peak grows in with increasing temperature as indicated in Fig. 6, suggesting that another new phase coexists with the usual gel phase in the high-temperature region. We will tentatively name this the G3 phase. The appearance of only one new peak in the wide-angle scattering requires that the G3 phase has hexagonal chain packing. The HWHM of the F peak goes from about twice the instrumental resolution at  $65^\circ\text{C}$  to resolution limited at higher temperatures, and this requires that the chains have little tilt ( $< 11^\circ$ ) with respect to the bilayer normal at the highest temperatures. Surprisingly, the chain packing density of the G3 phase is greater than

the usual gel phase; at 75°C, this new phase has an area per chain perpendicular to the chains  $A_c = 20.1 \text{ \AA}^2$ , compared to  $20.7 \text{ \AA}^2$  for the usual G1 gel phase, using the formula for  $A_c$  as in [6,7].

A time and temperature sequence of low-angle scattering is shown in Fig. 8. The peak near  $2\theta = 4.5^\circ$  is the highest observable order and it appears to be the fourth order of the lamellar stacking. Surprisingly, for most temperatures this fourth peak is larger than the second and third peaks and is often even better defined than the first peak. Because the fourth peak persists through all the temperature ranges, we suggest that it is associated with the G1 phase. This conclusion is further supported by the linear temperature dependence of the lamellar  $d$ -spacing (data not shown) that are calculated assuming the fourth peak to be the  $h = 4$  order peak for lamellar stacking. After the sample had been heated to 80°C and then returned to 35°C, trace 7 in Fig. 8 was promptly taken; the wide-angle data (not shown) had larger B and D peaks and smaller A and C peaks than those wide-angle data that corresponded to the first 35°C data (trace 2 in Fig. 8).

Trace 8 in Fig. 8 was also obtained at 35°C but after waiting 20 h after trace 7 was taken; the wide-angle scan (data not shown) had smaller B and D peaks and larger A and C peaks than the wide-angle scans for trace 7 and a similar wide-angle peak pattern to the one corresponding to trace 2. The four low-angle peaks in trace 8 of Fig. 8 index as lamellar orders 1–4 rather well. Trace 8 in Fig. 8 at 35°C is very similar to the trace at 45°C where there is only the G1 phase as determined by the wide-angle scattering. The G1 electron density profile (not shown) obtained

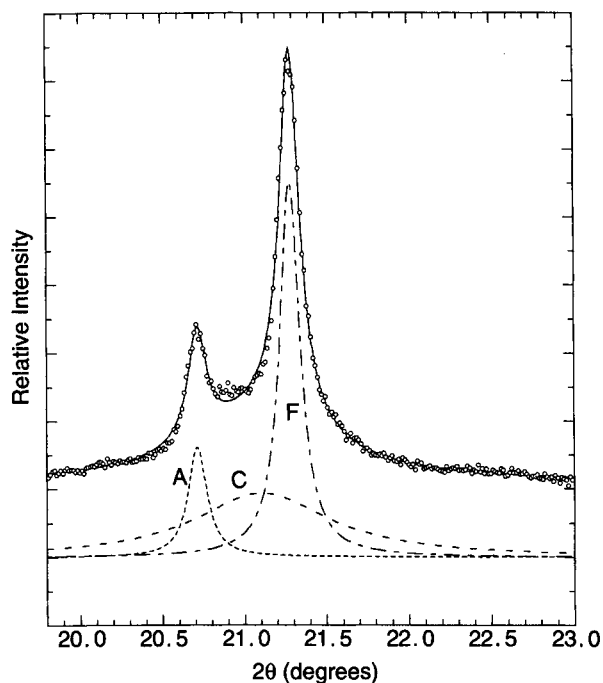


Fig. 7. Decomposition of wide-angle data (open circles) from  $C_{24}$  at 75°C into A, C and F components indicated by dashed lines. The solid line is the sum of the three components.

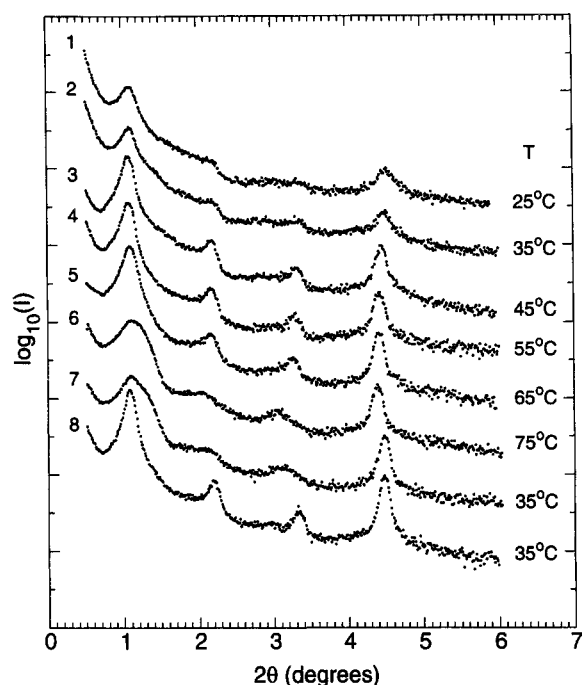


Fig. 8. Logarithm of low-angle data from the same sample of  $C_{24}$  in both the low- and high-temperature regimes. Data are shown in chronological order beginning at the top. Trace 8 was taken 20 h after trace 7.

from trace 8 by standard methods [16], with phases (— + —), is typical of gel phases.

In contrast to trace 8 of Fig. 8, the behavior of the first three peaks is more complex for some of the other traces. The broad, low second and third peaks in trace 7 in Fig. 8 do not index with the fourth peak or with the first peak and especially not with the shoulder on the first peak, which is the extra part of that peak compared to trace 8. In the high-temperature regime the low-angle data also show broadening and shifting of the second and third peaks (trace 6 in Fig. 8), accompanied by the onset and growth of the wide-angle F peak in Fig. 6. At 75°C, the third peak gives a  $d$ -spacing of about 86 Å if one were to assume that it is the  $h = 3$  order, but this is inconsistent with the  $d$ -spacing of 80 Å that is obtained from the fourth peak assuming that it is the  $h = 4$  order. The widths of the second and third peaks are about twice as broad as the instrumental resolution, while the fourth peak is resolution limited.

To study thermal reversibility of the G3 phase which gives rise to the F peak, the temperature of the sample was raised from 65°C to 80°C, then lowered back to 65°C, with the results shown in Fig. 9. Trace 1 in Fig. 9 (65°C) shows an initially small F peak compared to the A peak, signifying that the  $C_{24}$  sample is mainly in the usual G1 gel phase. Upon raising the temperature to 80°C, the AC peaks disappear and the F peak grows, indicating that the sample is then purely in the F phase. This transition is not immediately reversible as seen in traces 4 to 6 in Fig. 9. Although the AC peaks grow back upon reducing the temperature, they remain smaller than the F peak at 65°C,

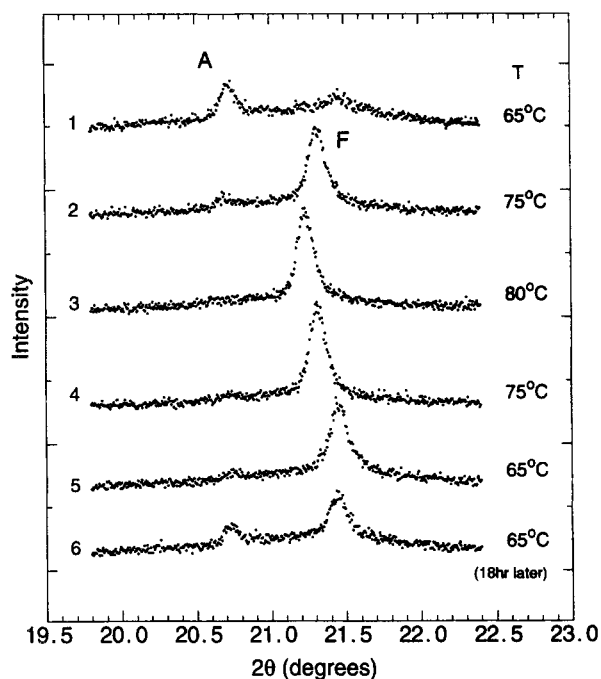


Fig. 9. Wide-angle scattering showing the time and temperature dependence of the A and F peaks for the same sample of  $C_{24}$ . Each trace was taken one hour after the preceding one with the exception of the last trace.

in contrast to trace 1, even after waiting nearly a day at 65°C. The dramatic differences between the data in Fig. 6 and in Fig. 9 are also consistent with having non-equilibrium in the high-temperature regime. It should also be mentioned that we found that long X-ray exposure of the lipid at high temperature induced phospholipid breakdown as determined by thin-layer chromatography (TLC), and so efforts were made to minimize such exposure. TLC on the sample in Fig. 9 showed 1% lysolecithin compared to a standard curve.

#### 4. Discussion

Compared to chain lengths  $n < 20$ , there appear to be two distinct novel phenomena occurring in the X-ray diffraction data from saturated longer chain phosphatidylcholines, in particular  $C_{24}$ . The first novel phenomenon is the appearance of extra scattering peaks, B, D and E at low temperature. The second is the appearance of an additional scattering peak F above 45°C. Only for temperatures 40–45°C does  $C_{24}$  have a reproducible, normal chain-tilted gel phase with only peaks A and C in the wide-angle region.

In the low-temperature regime,  $T < 40^\circ\text{C}$ , the intensities of the two extra peaks (B and D in Fig. 3) decrease in the same proportion, when temperature or sample history are varied, but the ratio of the A to B peaks varies widely. Furthermore, compared to the changes in relative intensities of the A and B peaks, there is relatively little shift in

each peak position with temperature (Fig. 4) compared to the separation between the peaks. This behavior strongly suggests the coexistence of two phases.

There is, however, a major thermodynamic difficulty with the explanation of the data in terms of coexisting G1 and G2 phases in the low-temperature regime. According to Gibbs' phase rule, in the presence of an excess water phase and at constant pressure, lipid bilayers composed of a single lipid component may exhibit two phase coexistence only at a single temperature if the system is in equilibrium. The apparent phase coexistence over wide temperature ranges in Figs. 4 and 6 is only permitted if the system is not in equilibrium. Of course, the existence of considerable hysteresis (compare traces 1 and 2 of Fig. 3) and transient behavior (compare the bottom two traces of Figs. 8 and 9) imply that the system is not in thermal equilibrium. This will be our tentative rationale for not rejecting, on thermodynamic grounds, the identification of the G2 and G3 phases that are only observed in coexistence with the G1 phase over wide temperature ranges. While the presence of non-equilibrium samples obviously makes it impossible to determine equilibrium phase diagrams, we nevertheless believe that the  $C_{22}$  and  $C_{24}$  lecithins have two additional chain-ordered phases, G2 and G3, which will be discussed in detail after this paragraph. The G1 phase that scatters into the A and C peaks would appear to be an ordinary gel phase, whose wide-angle  $d$ -spacings fit smoothly with the gel phase for shorter chain lengths  $n < 20$  (Fig. 2) and whose low-angle intensities yield a typical gel phase electron density profile. The only anomaly associated with the G1 phase is the appearance of the E peak near 35°C (trace 4 in Fig. 4).

Scattering into the B and D wide-angle peaks is interpreted as due to the G2 phase. Both the B and D peaks are resolution limited at 25°C. Such narrow lines require that the tilt angle be smaller than 11 degrees and that the intrinsic coherence length be larger than 500 Å. The fact that the B peak is larger than the D peak can be explained as an orthorhombic breaking of the hexagonal symmetry such that peak B is the sum of the (11) and (1 $\bar{1}$ ) peaks and peak D is the (20) peak. This is easily accomplished by stretching the hexagonal chain packing lattice along the (01) direction; this is perpendicular to the direction of stretching for the G1 phase where the (20) peak appears at lower scattering angles than the (11) peak. This difference may also be characterized by different signs for the distortion parameter defined by Sirota et al. [17]. This indexing of the G2 phase wide-angle peaks is consistent with the appearance of two additional weak wide-angle peaks (Fig. 5) whose intensities are proportional to the B and D peaks and that index as (31) and (02). The absence of any peaks between the low-angle peaks and the B peak and of any peaks whose sum of indices is odd suggests that the G2 phase should be described as another gel phase rather than a subgel phase. This conclusion is also consistent with the observations of Lewis et al. [2] that the incubation time for

initiating formation of subgel phases increases dramatically with chain length, reaching the order of weeks for  $C_{22}$ . The one disturbing aspect of this interpretation of the wide-angle scattering of the G2 phase is that the ratio of intensities of the B peak to the D peak is closer to four than to the value of two that one would expect if the B peak is the doubly degenerate (11) and ( $\bar{1}\bar{1}$ ) peaks. As has been mentioned previously [7], this intensity could vary by 40%, although this would require chain packing similar to crystal or subgel phases. Hopefully, other techniques, such as infrared spectroscopy, can clarify these possibilities.

The area per chain  $A_c = 18.5 \text{ \AA}^2$  of the G2 phase at 25°C yields, when multiplied by 1.27 Å, the volume per methylene  $V_{CH_2} = 23.6 \text{ \AA}^3$ . These values are smaller than the corresponding values for the  $C_{24}$  gel phase G1 with  $A_c = 19.3 \text{ \AA}^2$  and  $V_c = 24.5 \text{ \AA}^3$  also at 25°C; this means that the G2 phase is denser than the G1 phase, which is consistent with it becoming more pronounced at lower temperatures. The apparently small tilt angle in the G2 phase requires, however, that the area/headgroup  $A = 2A_c = 37 \text{ \AA}^2$  be considerably smaller than for the G1 phase for which  $A = 47\text{--}48 \text{ \AA}^2$  [6]. One possibility for alleviating headgroup crowding is to offset the headgroups along the bilayer normal in an alternating pattern; this kind of pattern has been suggested for the subgel phase of DPPC ( $C_{16}$ ) [11]. This kind of packing would presumably cost free energy in the headgroup region and gain free energy in the hydrocarbon chain region. The longer chains in  $C_{24}$  would make this option relatively more favorable than for shorter chains. Another possibility to avoid headgroup crowding in the G2 phase would be untilted interdigitated lipids because then  $A$  would be essentially  $4A_c$ , even larger than the  $A = 2A_c/\cos\theta$ . Interdigitation would be expected to decrease the low-angle lamellar  $d$ -spacing [18].

The low-angle pattern of the G2 phase is complicated by the history dependence. One possibility is that the first order low-angle peak is the shoulder at higher angle to the usual G1 first order peak (see trace 7 in Fig. 8, which corresponds in the wide-angle region to more G2 phase). This would be consistent with the G2 phase being interdigitated with  $d$ -spacing about 65 Å compared to a  $d$ -spacing of about 80 Å for the G1 phase. Comparison of trace 7 in Fig. 8 with trace 8, which corresponds to more G1 phase, suggests that the G2 phase is associated with the broad second and third peaks. Unfortunately, these broad peaks do not index with the shoulder on the  $h = 1$  peak, nor do they index with either the  $h = 1$  peak or with the well-defined  $h = 4$  peak that appears to be associated with the G1 phase. Therefore, the low-angle pattern for the G2 phase is unclear at present. We have considered the possibility that the G2 phase is not multilamellar, but hexagonal or cubic phases would seem to be inconsistent with the sharp wide-angle peaks B and D.

In contrast to the uncertainty in the low-angle pattern for the G2 phase, the G1 phase appears to be rather well

characterized. The G1 phase corresponds to the four sharp peaks in trace 8 in Fig. 8 which are similar to the four peaks at 45°C in trace 3 in Fig. 8 for which the wide-angle pattern has only the A and C peaks of the G1 phase. The electron density profile obtained from traces 3 or 8 of Fig. 8 indicates trans-bilayer headgroup spacings of roughly 58 Å. This is consistent with  $C_{24}$  chains tilted at about 36 degrees as will be discussed in detail in another paper. The electron density profile also indicates the usual terminal methyl trough in the center of the bilayer.

In the high-temperature regime,  $T > 45^\circ\text{C}$ , there appears to be a different new phase G3, identified by the F peak, that coexists with the usual G1 phase over a wide temperature range. This coexistence has the same thermodynamic difficulties as the G2/G1 phase coexistence. We have also observed time dependence in the proportions of this coexistence (see Fig. 9), so we believe that the coexistence is due to non-equilibrium and not due to any fundamental difficulty with Gibbs' phase rule.

The G3 phase has only one rather symmetrical F peak in the wide-angle region. This indicates that this is a phase with basically hexagonal packing of the chains. The relative sharpness of this peak suggests that the chains in this phase have rather small tilt angles. A consequence is that the headgroup area  $A$  is nearly  $2A_c = 40.16 \text{ \AA}^2$ . As with the G2 phase, this value of  $A$  is rather small for lecithins. A possible resolution of this problem is that the G3 phase might be a ripple phase; if so, then the effective headgroup area is larger, being proportional to the amplitude of the ripples and inversely proportional to the ripple repeat distance. Support for the possibility that G3 is a ripple phase include:

1. G3 has hexagonal chain packing, as in the ripple phase of shorter chain length lipids [9].
2. The  $d$ -spacing measured from the second and third peaks at 75°C in Fig. 8 is 86 Å. This is about 6 Å larger than the  $d$ -spacing of 80 Å measured from the fourth peak that we interpret as the fourth order of the G1 phase. This difference agrees with the  $d$ -spacing differences between the gel phase and the ripple phase of the shorter chain lengths.
3. The widths of the second and third peaks are about twice as broad as the instrumental resolution, while the fourth peak is resolution limited.

Previous ripple phase studies [19] show that as the chain length increases, and as full hydration is reached, the ripple scattering peaks weaken, broaden, and intermingle with the lamellar peaks. When the resolution is not high enough, one would expect to see broad peaks composed of ripple and lamellar peaks.

We have considered various explanations for the observed non-equilibrium behavior. High temperature annealing could induce chemical disintegration of the hydrated lipid. However, this would be expected to inhibit G2 phase formation because impurities usually retard formation of more ordered phases, such as the subgel phase in DPPC

[14], but high temperature results in more G2 phase. A different non-equilibrium hypothesis that we have explored involves the possibility of some extra variable that makes the sample intrinsically heterogeneous. A particular way to realize this general hypothesis would be to have a distribution in the size  $R$  of the multilamellar vesicles and to postulate that larger vesicles have higher temperatures for G2  $\rightarrow$  G1 transitions. There are two trends in our observations that are consistent with this hypothesis. First, we have noticed that there is usually more G1 phase (larger AC peaks) in the low-temperature regime below 40°C upon first loading a sample into capillaries using a Hamilton syringe, where the shearing forces might break up large MLVs. Second, raising the temperature to 80°C could anneal the sample to larger MLVs, thereby explaining the differences between traces 1 and 2 in Fig. 3. The occurrence of more G2 phase in trace 3 of Fig. 3 would be due to formation of large MLVs in the capillary. However, we also have data that do not fit neatly into this hypothesis, so we will not claim to have established any comprehensive model for the non-equilibrium phase coexistence.

Despite these non-equilibrium complications in preparations of long chain lecithins, our data clearly indicate that they have a propensity for forming phases in addition to the usual gel phase. These new phases could be interesting to elucidate new ways for lipids to interact. Additional experimental techniques should be employed to supplement the X-ray data in this paper and to test our tentative suggestions for the nature of the G2 and G3 phases. Finally, recognizing the existence of these anomalous phases is essential in order to complete future work on the systematic temperature and chain length studies of the usual G1 gel phase of saturated lecithin bilayers.

### Acknowledgements

We thank R.G. Snyder for informing us prior to publication of infrared absorption data that also indicates new

phase behavior in these long chain lipids. This research was supported by the US National Institutes of Health grant GM-44976.

### References

- [1] Nagle, J.F. and Wilkinson, D.A. (1978) *Biophys. J.* 23, 159–175.
- [2] Lewis, R.H.A.H., Mak, N. and McElhaney, R.N. (1987) *Biochemistry* 26, 6118–6126.
- [3] Huang, C., Wang, Z.-Q., Lin, H.-N., Brumbaugh, E.E. and Li, S. (1994) *Biochim. Biophys. Acta* 1189, 7–12.
- [4] Cevc, G. (1991) *Biochim. Biophys. Acta* 1062, 59–69.
- [5] Wilkinson, D.A. and Nagle, J.F. (1984) *Biochemistry* 23, 1538–1541.
- [6] Tristram-Nagle, S., Zhang, R., Suter, R.M., Worthington, C.R., Sun, W.-J. and Nagle, J.F. (1993) *Biophys. J.* 64, 1097–1109.
- [7] Sun, W.-J., Suter, R.M., Knewton, M.A., Worthington, C.R., Tristram-Nagle, S., Zhang, R. and Nagle, J.F. (1994) *Phys. Rev. E* 49, 4665–4676.
- [8] Hentschel, M. and Hosemann, R. (1983) *Mol. Cryst. Liq. Cryst.* 94, 291–316.
- [9] Hentschel, M. and Rustichelli, F. (1991) *Phys. Rev. Letters* 66, 903–906.
- [10] Smith, G.S., Sirota, E.B., Safinya, C.R. and Clark, N.A. (1988) *Phys. Rev. Letters* 60, 813–816.
- [11] Ruocco, M.J. and Shipley, G.G. (1982) *Biochim. Biophys. Acta* 691, 309–320.
- [12] Ruocco, M.J. and Shipley, G.G. (1982) *Biochim. Biophys. Acta* 684, 59–66.
- [13] Stumpel, J., Eibl, H. and Nicksch, A. (1983) *Biochim. Biophys. Acta* 727, 246–254.
- [14] Tristram-Nagle, S., Suter, R.M., Sun, W.-J. and Nagle, J.F. (1994) *Biochim. Biophys. Acta* 1191, 14–20.
- [15] McIntosh, T.J. (1980) *Biophys. J.* 29, 237–245.
- [16] McIntosh, T., Magid, A.D. and Simon, S.A. (1989) *Biochemistry* 28, 17–25.
- [17] Sirota, E.B., King, H.E., Singer, D.M. and Shao, H.H. (1993) *J. Chem. Phys.* 98, 5809–5824.
- [18] McIntosh, T.J., Simon, S.A., Ellington, J.C. and Porter, N.A. (1984) *Biochemistry* 23, 4038–4044.
- [19] Wack, D.C. and Webb, W.W. (1989) *Phys. Rev. A* 40, 2712–2730.